University of Tabriz

Investigating the Effects of Geometric Parameters of Buckling Restrained Braces on the Cyclic Behavior of Buckling Restrained Braced Frames

Ehsan Dehghani [a,*], Narges Babaei [b], Alireza Zarrineghbal [c]

[a] *Assistant Professor, Department of Civil Engineering, University of Qom, Qom, Iran*
[b] *PhD Student, Department of Civil Engineering, University of Shahid Bahonar, Kerman, Iran*
[c] *PhD Candidate, School of Civil Engineering, College of Engineering, University of Tehran, Tehran, Iran*

ABSTRACT:

Today, the buckling-restrained bracing frames (BRBFs) are widely used as a new system contributing to the absorption of a high amount of energy through yielding of the buckling-restrained brace (BRB) core when exposed to compression and tension. The relatively high cost of exploitation of this system has prompted researchers to seek for ways to reduce the costs while providing seismic performance. The present study was carried out to investigate the effect of the ratio of the yielding segment cross-sectional area to the elastic segment cross-sectional area as well as the length of the yielding segment to the total length of the BRB core on energy absorption demand of these braces in different stories of the BRB frames. For this purpose, two 5-and-10-story BRB frames have been modeled in Open Sees software, then the nonlinear time history analysis was performed on these frames under seven earthquake records. Using the results of the analysis, the energy absorption demand of braces on different stories with different ratios of the yielding segment cross-sectional area to the elastic segment cross-sectional area as well as the length of the yielding segment to the total length of the BRB core has been calculated. The results indicated that the variation of these ratios in the BRB can be effective in the amount of energy absorption demand of, in addition, the nature of this effect depended on the braced story in the BRB frame. However, the effect of stiffness modification factor on the uniformity of the energy absorption demand of braces in different stories is insignificant compared to the changes in the cross-sectional area of braces in different stories.

KEYWORDS:

Buckling-restrained brace, Energy absorption demand, Cyclic behavior, Buckling-restrained bracing frame, Stiffness modification factor.

1. Introduction

As one of the main lateral force-resisting members, braces can effectively enhance lateral rigidity of framed structures (Jiu Jia et al. 2019), however, the ductility and energy dissipation potential of steel bracing structures are limited under earthquakes (Jia et al. 2014). The buckling-restrained bracing (BRB) frames are an advanced type of concentric braced frames (CBFs) capable of solving the buckling problem and improving the ductility and stiffness of these frames (Hosseinzadeh et al. 2016). BRB frames have been developed in Japan since 1980 (Watanabe et al. 1988) and were widely used after the Kobe earthquake in 1995. These frames were widely used in the United States after the Northridge earthquake

in 1994 (Clark et al. 1999) and accepted in the American Institute of Steel Construction (AISC) standard (2010). The stable nonlinear behavior of the BRBs makes them as elements acting as an energy dissipation tool during an earthquake (Mahdavipour et al. 2014).

BRBs are composed of a ductile steel core yielding in tension and compression. The steel core is placed in a steel casing filled with concrete or mortar (Dehghan et al. 2016). In addition, an unbonded layer is embedded between them to prevent the transfer of axial force from the steel core to the surrounding concrete (Bosco et al. 2013). As illustrated in Fig. 1, the bracing core consists of five parts, including: a restrained part yielding in tension and compression, two parts responsible for the force transfer; these parts are restrained, do not yield, and have a cross section larger than the yielded part, and the other two parts including the joints following the steel core, but more protuberant than the outer box, hence they are not restrained. This part does not yield and provides the conditions of connection to the structure (Lopez et al. 2004).
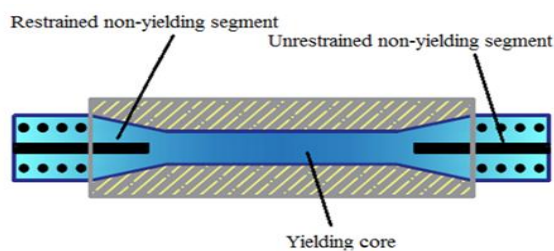
Fig. 1. Different parts of the buckling-restrained bracing (BRB) core

Finding a solution to improve the seismic behavior of BRB frames while improving the cost of using these frames is an issue of great importance which has attracted the attention of numerous researchers. For example, the pseudo-static tests (PSTs) of a buckling-restrained braced composite frame (BRBCF) system consisting of concrete-filled circular hollow section (CHS) steel columns, steel beams and BRBs were tested. The fracture and buckle of CHS steel tubes at the first story base indicated the thickness of CHS steel tube of composite columns in BRBCF should be enlarged to avoid the early failure of composite columns (Jia et al. 2014), but in this research, BRBFs have been used.

In a study the behavior of buckling restrained braces has been investigated by considering different types of surrounding covers. According to results, applying steel with high ductility promotes the energy dissipation of the brace (Rahai et al. 2009). In another study, the effects of parameters such as the width of the gap between the core and

the encasing concrete and the cross section of the core on cyclic behavior of buckling restrained brace have been investigated (Karimi et al. 2008). As another example, a study is focused on the analytical evaluation of hysteretic response of BRBs of varying lengths using finite element (FE) software. Results show that a reduction in the yielding core segments of BRBs results in the improved elastic axial stiffness of BRBs which may help in controlling the excessive residual drift response (Pandikkadavath et al. 2016). Since the BRB is a non-prismatic element, the various ratios of the yielding segment cross-sectional area to the elastic segment cross-sectional area as well as the length of the yielding segment to the total length of the BRB core must be taken into account in the design of this element. In this study, for BRB frame, it has been tried to determine the effect of variation of these ratios in BRBs on the energy absorption demand in these braces on different stories.

2. Cyclic behavior and energy dissipation of BRB

Since earthquake has a reciprocal nature, the structure experiences the loading and unloading properties repeatedly during the earthquake. If the force-deformation diagram of the structure during the earthquake is plotted, then the resulting graph is the hysteresis loop.

Typical steel braces rapidly experience global buckling under compressive loads, hence their load-bearing is stopped, and the hysteresis loop of these braces is very small in the compression area. However, the BRB braces tolerate a local (sinusoidal) buckling inside the steel casing under compressive loads, hence dramatically increasing the load-bearing capacity of the system in the compression area. Fig.2 demonstrates a comparison between the behavior of a BRBF and a concentric braced frame (CBF) in a loading cycle.
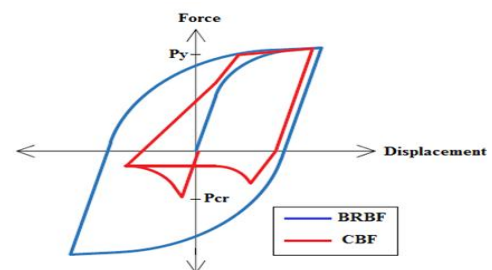
Fig. 2. Comparison of hysteresis loop of concentric braced frames (CBFs) and buckling-restrained braced frames (BRBFs)

In CBFs, the buckling of the brace is inevitable, causing a drop in strength and stiffness, which in some cases can cause a failure concentration on a certain number of stories, however the drop of

strength to compression and the reduction of stiffness, which are of the drawbacks of the conventional brace, are not observed in the BRB (Bruneau et al. 2011) and BRBs have a stable and full hysteretic curve (Qu et al. 2019).

The area under the force-deformation curve indicates the absorption or dissipation of energy in the structure. In other words, the area under loading and unloading curves represents the energy dissipation in the structure. In the elastic mode, loading and unloading are carried out within the linear region, hence the hysteresis loop does not form, and therefore there is no dissipation of energy. When the structure enters the plastic area, the loading and unloading hysteresis loops will be formed, and the internal area of the graph will be the same as the energy dissipated in the plastic mode (Raissi et al. 2017). If a BRB is subjected to the axial cyclic tensile force, the desired force-deformation curve will be as depicted in Fig. 3. The total energy transferred to the BRB is the shaded area of the trapezium. In addition, the triangular red shaded area represents the energy returned due to unloading, and the equilateral area with the remaining blue shade indicates the energy absorbed by the brace. The larger the equilateral area, the higher the absorbed energy by the brace.
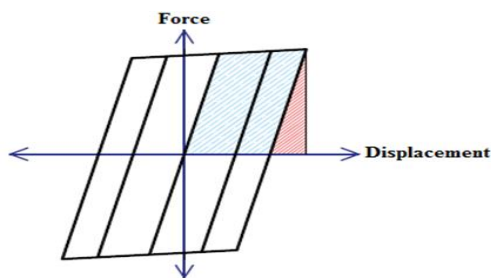
Fig. 3. Desired force-deformation curve of a buckling-restrained brace (BRB)

3. Description, modeling, and analysis of the buildings under study

In this study, two 5-and-10-story buildings with a BRB frame in one direction with the same plan as shown in Fig. 4 have been used. The height of the stories and the length of the spans are 3 and 6 meters, respectively. The soil of the area is assumed to be of type II and the structure is located in a zone with a high relative risk according to Standard 2800 (2015). The frames have been modeled two-dimensionally due to the regularity of the frames in the plan and height (Fig. 4). The buildings have been designed in the ultimate limit method in accordance

with the AISC360-10 (2010), which is highly similar to the Iranian National Building Regulation, Part-10 (2013). Design seismic parameters including Response modification coefficient (R), over strength factor (Ω), and the deflection amplification factor, (Cd) according to ASCE7-10 code (2010) were considered as 2, 7, and 5.5, respectively. In the present study, the Iranian National Building Code, Part 6 (2013) and standard No.2800, version 4 have been used for gravitational and seismic loadings, respectively.

The modeled and analyzed 5-and-10 story BRB frames have been demonstrated in Fig. 4.b and Table 1 shows the sections designed for these frames. The 5-and-10 story BRB frames shown in Fig. 4.b were modeled in Open Sees software and then the nonlinear time history analysis was performed on these frames under seven earthquake records. All joints were modeled as articulated.

(a)

(b)
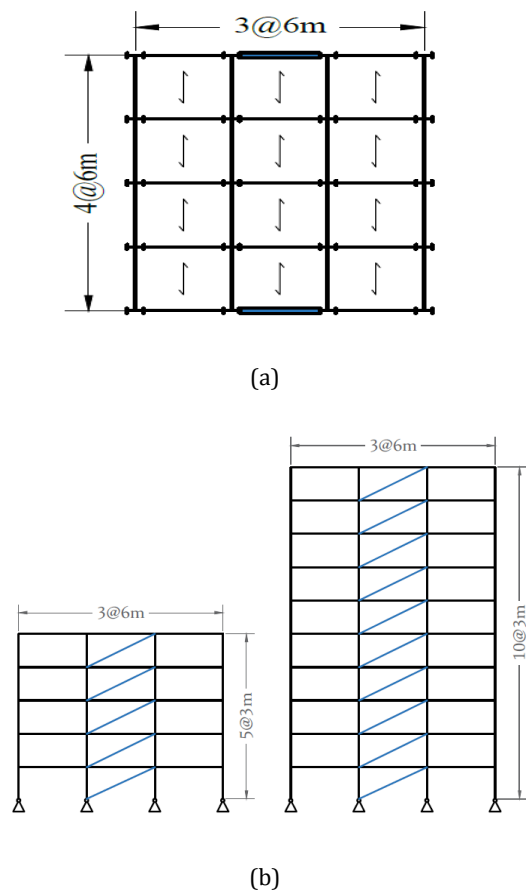
Fig. 4. Building plan and 5-and-10 story frames under study: (a) Building plan, (b) 5-and-10 story frames

Table 1. The sections designed for 5-and-10 story BRB frames

Frame	Story	Column cross section		Beam cross section		Brace cross section
		Middle columns	Lateral columns	Middle Beam	Side Beam	
10-story	1	H400×509-1	HE300A-1	IPE750×137	IPE400O	StarBRB11
	2	H400×422	HE300A	IPE750×137	IPE400O	StarBRB10.5
	3	H400×383	HE280A	IPE750×137	IPE400O	StarBRB10.5
	4	H400×314	HE260A	IPE750×137	IPE400O	StarBRB9.5
	5	H400×262	HE240A	IPE750×137	IPE400O	StarBRB9
	6	HE550B	HE220A	IPE750×137	IPE400O	StarBRB8
	7	HE450A	HE200A	IPE750×137	IPE400O	StarBRB7
	8	HE320A	HE180A	IPE750×137	IPE400O	StarBRB5.5
	9	HE240A	HE140A	IPE750×137	IPE400O	StarBRB4
	10	HE160A	HE120A	IPE750×137	IPE400O	StarBRB2
5-story	1	HE550B	HE220A	IPE400O		StarBRB6.5
	2	HE360B	HE200A	IPE400O		StarBRB6
	3	HE280B	HE180A	IPE400O		StarBRB5
	4	HE240A	HE140A	IPE400O		StarBRB4
	5	HE160A	HE120A	IPE400O		StarBRB2

The fiber sections were used for modeling the beam and column members and their nonlinear behavior was defined by the steel02 material. The members of the beams and columns were defined as nonlinear beam-column, so that their nonlinear behavior is taken into account in nonlinear analyses.

3.1. Parametric design equations

The important point in the modeling of the BRB in software is that the BRB is a non-prismatic member with different parts, including the yielding core, transfer section, and the joints section each with a different cross-section. Typically, the BRB sections are modeled as prismatic sections with a cross section equal to the area of the steel core. Therefore, the stiffness of the brace must be modified to consider the effect of other parts; this is usually fulfilled through multiplying the cross section of the steel core or modulus of elasticity by the stiffness modification factor (KF). KF is defined as the ratio of the elastic stiffness of the non-prismatic BRB element to the elastic stiffness of the prismatic element with the steel core cross-section. KF can be calculated using the Eq. (1):

$$KF = \frac{L}{L_i + A_i\left(\frac{L_{con}}{A_{con}} + \frac{L_{tr}}{A_{tr}}\right)} \quad (1)$$

Where L, L_i, A_i, L_{tr}, A_{tr}, L_{con}, and A_{con} are the total length of the brace, the length of the yielded area, cross-sectional area of the yielded area, length of the transfer area, cross-sectional area of the transfer area, length of the connection area, and cross-sectional area of the connection area.

KF depends on factors like the geometry of the BRB including its size, length, and shape, details of connections, and even the BRB constructor, and has a specified range of 1.3 to 1.7 (Kersting et al. 2015). In addition to modeling the BRB as a prismatic member and using the stiffness modification factor, its modeling directly as a non-prismatic member

using the finite element method program is a reliable method. To compare this complete model with a simplified model, Rahnavard (Rahnavard et al. 2018) used the ABAQUS finite element method program and proposed an intended simple model such as core and springs. A good agreement was observed between the two results with 5% difference.

Since BRB is a non-prismatic member, its different parts can have different lengths and areas (Fig. 5). In this study, the BRBs are designed according to AISC360-10 for different stories of 5-and-10 story frames with different geometric parameters α (the yielding segment cross-sectional area to the elastic segment cross-sectional area) and β (length of the yielding segment to the total length of the core) according to Table 2 were modeled in the Open Sees software, then the nonlinear time history analysis was performed on them under seven earthquake records.
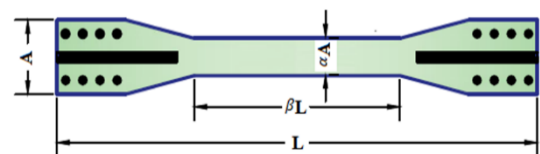
Fig. 5. Geometric parameters of the buckling-restrained brace (BRB)

Table 2 stiffness modification factor and different ratios of α and β for the buckling-restrained brace (BRB) in 4 different modes

Brace sample	KF	β	α
1	1.3888	0.6	0.3
2	1.6666	0.5	0.2
3	1.5384	0.5	0.3
4	1.4705	0.6	0.2

In this study, the BRBs were modeled with Truss element. Therefore, in order to consider the real stiffness of the BRB as a non-prismatic member in the modeling, modulus of elasticity of the braces was multiplied by the stiffness modification factor (KF). The response of the braces can be approximately modeled with a bi-linear representation (Fig. 6) to capture the maximum forces, displacements and energy dissipation in the braces (Carden et al. 2006). The steel02 material was exploited for the modeling of nonlinear behavior of braces.
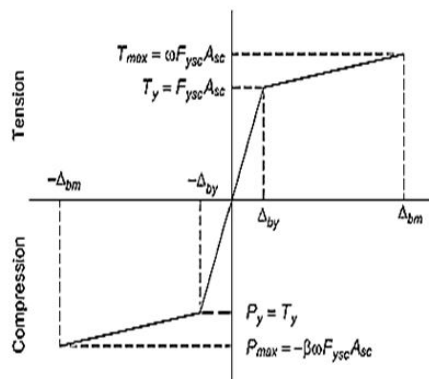
Fig. 6. Ideal diagram of force-displacement in buckling-restrained brace (AISC 341, 2010)

In order to perform the nonlinear time history analysis of the frames, the horizontal components of the seven earthquake records that the characteristics of which were in accordance with Table 3 and matched with the range of the standard 2800, were used.

4. Models analysis results

In this study, two 5-and-10-story frames were modeled in the Open Sees software. The BRB designed for each frame were modeled with 4 different ratios α and β according to Table 2. The nonlinear time history analysis was performed on each model under seven earthquake records. The hysteresis loop can be plotted for each of the braces using the results of the analyses. Using the obtained hysteresis loops, the energy absorption demand can be obtained for each of the braces.

The hysteresis loops of the BRBs of the first and fifth stories of the 5-story frame under Chi Chi and Loma Prieta earthquakes with different ratios of α and β according to the rows 1 and 2 of table 2 are illustrated in Fig. 7.

In Fig. 7.a, b the hysteresis loops of the BRB of the first story of the 5-story frame resulting from the nonlinear time history analysis under Chi Chi and Loma Prieta earthquakes for two cases in which the BRBs have different ratios of α and β in accordance with rows 1 and 2 of Table 2, have been compared. The StarBRB6.5-1 has higher ratios of α and β and lower KF and hence, the lower elastic stiffness compared to the StarBRB6.5-2 BRB. Similarly, in Fig. 7.c, the hysteresis loops of the BRB of the fifth story of this frame is also shown for two cases where the BRB has different ratios of α and β in accordance with rows 1 and 2 of Table 2. The hysteresis loops in Fig. 7.a, b also indicate that the StarBRB6.5-1 BRB has less elastic stiffness than StarBRB6.5-2, in addition, the hysteresis loops of Fig. 7.c, d, which is related to the BRB of the fifth story, shows that StarBRB2-1 has less elastic stiffness in comparison to StarBRB2-2. The difference in the stiffness of the braces in cases 1 and 2 in the first story where the BRB has a larger cross-section, is more than the stiffness difference of the braces in the fifth story in the 1 and 2 cases.

Table 3. Characteristics of earthquake records used

Row	Event	*PGA* (g)	Magnitude	Station	Distance (km)	Year of occurrence
1	Tabas	0.85	7.35	Tabas	2.05	1978
2	Chi Chi	0.96	7.62	CHY080	2.69	1999
3	Imperial Valley-02	0.31	6.95	El Centro Array #9	6.09	1940
4	Kobe	0.69	6.9	Takarazuka	0.27	1995
5	Cape Mendocino	1.49	7.01	Cape Mendocino	6.96	1992
6	Loma Prieta	0.54	6.93	Capitola	15.23	1989
7	Northridge	0.55	6.69	Arleta - Nordhoff Fire Sta	8.66	1994
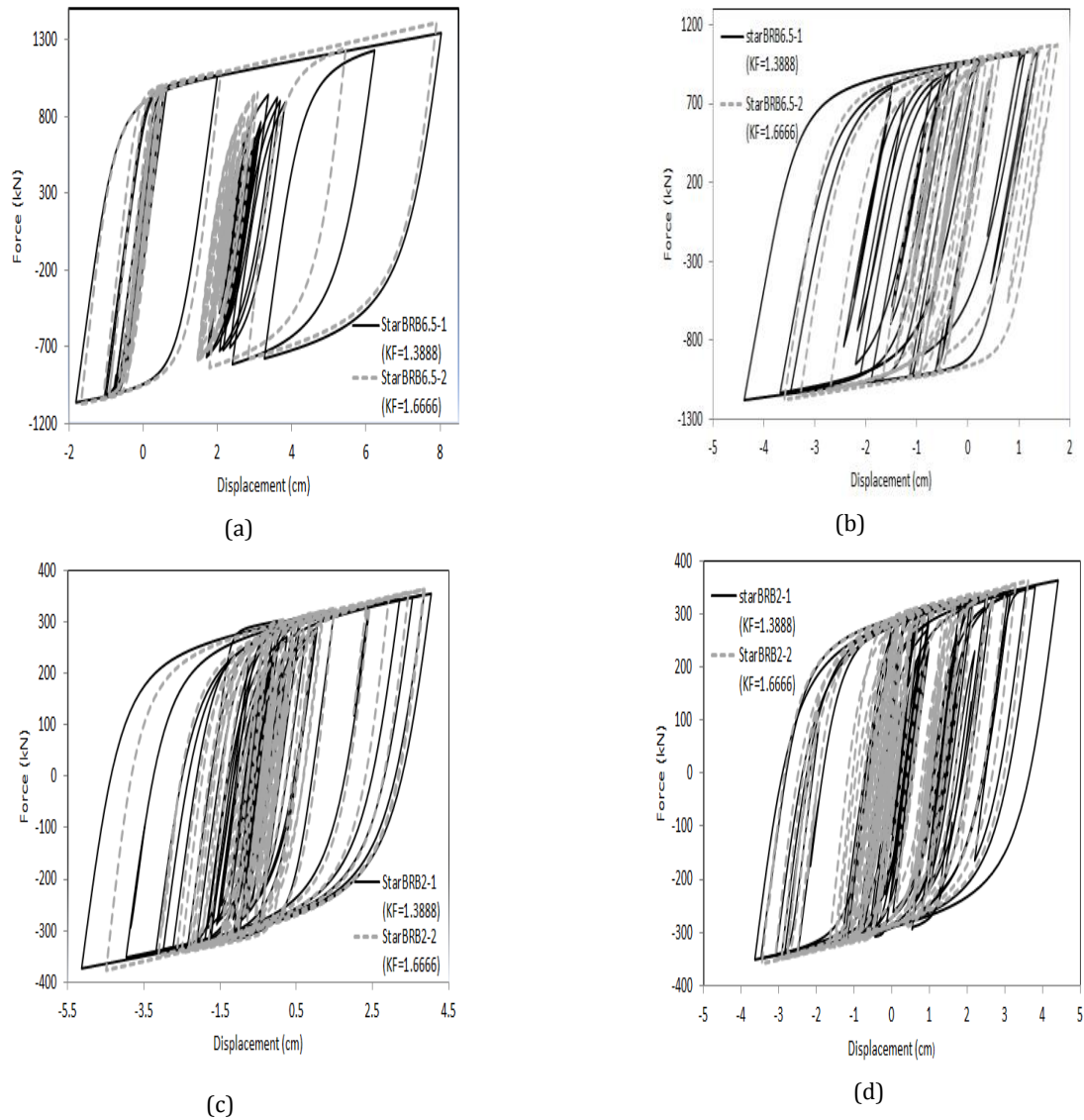
Fig. 7. Hysteresis loop of the buckling-restrained braces (BRBs) of the 5-story frame under Chi Chi and Loma Prieta earthquake: (a) First story brace (Chi Chi), (b)First story brace (Loma Prieta), (c) Fifth story brace (Chi Chi), (d) Fifth story brace (Loma Prieta)

Moreover, for the BRB of the first and the tenth stories of the 10-story frame, the hysteresis loop of the BRB has been plotted in Fig. 8 under Chi Chi and Loma Prieta earthquakes for two cases in which the BRB has different ratios of α and β in accordance with rows 1 and 2 of Table 2.

Hysteresis loops exhibit more elastic stiffness of StarBRB11-2 compared to StarBRB11-1, as well as more elastic stiffness of StarBRB2-2 than StarBRB2-

1. For hysteresis loops presented in Fig. 7, 8, the energy absorption demand which is the area under the hysteresis loop, has been calculated and presented in table 6. The energy absorption demand of BRB of the first story was higher in both frames when the BRB with the higher elastic stiffness was used. For BRB of the last story in both frames, the use of StarBRB2-1 with less elastic stiffness than StarBRB2-2 has resulted in more energy absorption

(a)

(b)

(c)

(d)
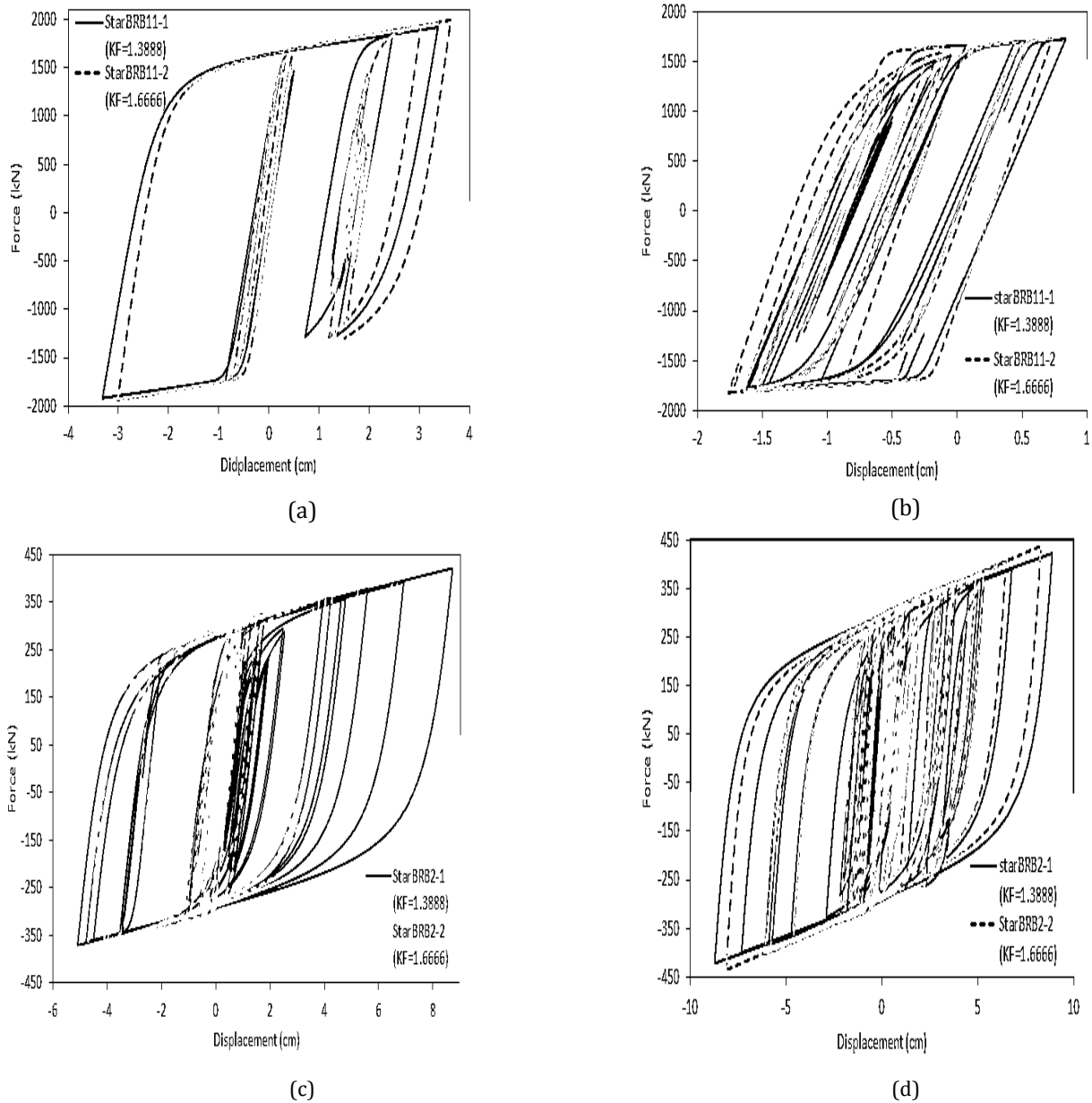
Fig. 8. Hysteresis loop of the buckling-restrained braces (BRBs) of the 10-story frame under Chi Chi and Loma Prieta earthquakes: (a) First story brace (Chi Chi), (b) First story brace (Loma Prieta), (c) Tenth story brace (Chi Chi), (d) Tenth story brace (Loma Prieta)

Table 4. Energy absorption demand and elastic stiffness of buckling-restrained braces (BRBs) of the first and last stories of the 5-and-10-story frames

Frame	Story	Brace	Elastic stiffness of BRB (kN/m)	Energy absorption demand of BRB under Chi Chi earthquake (kN.m)
5-story	First	StarBRB6.5-1	182165.87	252.65
		StarBRB6.5-2	218604.29	272.19
	Fifth	StarBRB2-1	56084.48	236.79
		StarBRB2-2	67302.99	215.86
10-story	First	StarBRB11-1	308682.02	187.94
		StarBRB11-2	370427.31	204.5
	Tenth	StarBRB2-1	56084.48	336.45
		StarBRB2-2	67302.99	316.18

In the present study, the energy absorption demand of BRBs of different stories of the two frames under study was studied in 4 states in which the braces had different ratios of α and β in accordance with table 2, and calculated under 7 earthquake records; the results for the average of the 7 earthquake records are depicted in Fig. 9.

(a)

(b)
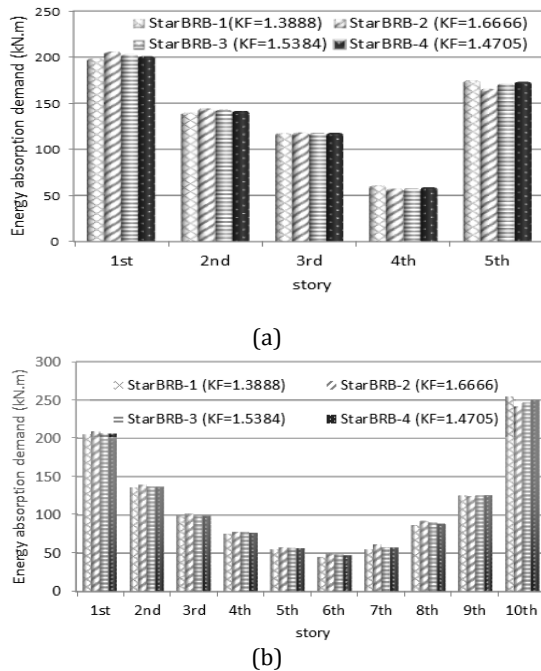
Fig. 9. Energy absorption demand of braces of different stories of the 5-and 10-story frames with different ratios of α and β for the average of 7 earthquake records: (a) 5story frame, (b) 10-story frame

As it can be observed in Fig. 9, the highest energy absorption demand in the first story of both frames has taken place when the BRB has been used with different α and β ratios according to the second row of Table 2 (StarBRB-2). The second row of Table 2 has the lowest value for α and β ratios, hence leading to the highest KF and therefore the highest elastic stiffness for the brace. On the first story of the both frames, the least energy absorption demand is related to the case where the BRB has been used with ratios presented in row 1 of Table 2 (StarBRB-1). Row 1 of the table includes the highest value for the ratios α and β which causes the least KF and elastic stiffness for the brace. On the first story, both BRB frames produce the highest to the lowest energy absorption demands with ratios presented in rows 2, 3, 4 and 1 of Table 2, respectively. These BRBs also have the highest to the lowest KF, respectively. Therefore, it can be concluded that in the first story of the two frames studied, the less KF and elastic stiffness, and hence lower energy absorption demand can be created for the brace using BRBs with higher ratios of α and $\beta.$ This trend continues up to the third story and eighth story of

the 5-story and 10-story frames, respectively, except that the difference in the energy absorption demand with the least and the highest KF is lowered moving toward higher stories. On the fourth story of the 5-story frame and the ninth story of the 10-story frame, the energy absorption demand has been obtained slightly higher for the brace with a lower KF. On the fifth story of the 5-story frame and the tenth story of the 10-story frame, this difference is greater and the energy absorption demand for the brace with the lowest KF is more than the energy absorption demand with more difference relative to the bottom story in the case where the brace has the highest KF. It can be concluded that in the frames under study, the use of braces with a higher KF can create less energy absorption demand for the brace in the upper stories. However, Figure 9 shows that the difference in demand for energy absorption for the four different states of bracing for all stories is insignificant compared to the difference in energy absorption demand of braces of different stories. Fig. 9 shows that the energy absorption demand of middle stories bracing is lower than the first and last stories. By changing the cross-sectional area of designed bracings, and choosing a larger cross-sectional area for bracings of stories demanding more energy absorption, the energy absorption demand of braces in different stories can become more uniform (Dehghani et al. 2018). But as shown in Fig. 9, compared to the changes in the cross-sectional area of bracing, the changes in the KF coefficient cannot have a significant effect on the uniformity of the energy absorption demand of braces in different stories.

Using the results of nonlinear time history analyzes with each of the 7 earthquake records, the maximum drift value was also obtained for each story. Fig. 10 shows these drift values for the average of 7 earthquake records and for different KF values according to Table 4 in the different 5-story frame stories.
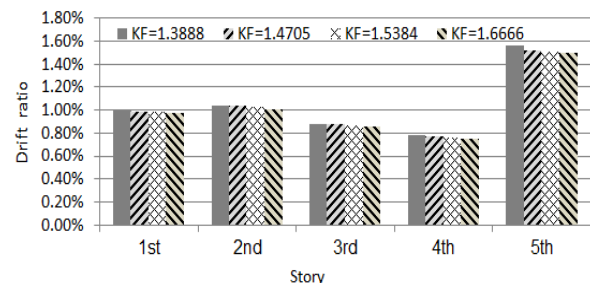
Fig. 10. Drift ratio of different stories of the 5 story frames with different ratios of α and β for the average of 7 earthquake records

As shown in Fig. 10, increasing the KF value has reduced the amount of drift in the different stories, however, the difference of one story drift due to different KFs is much less than the drift difference in the different stories of frames.

5. Conclusions

In this paper, two steel structures of 5-and-10 stories with the BRB frame in one direction were exposed to the gravitational and lateral loading according to the Iranian National Building Code, Part 6 and Iranian 2800 code, moreover, designing of sections of the beams and columns and the braces was performed in accordance with the AISC360-10 code. The 5-and-10 story frames were modeled in two-dimensional form in the Open Sees software. The BRBs designed for frames were modeled with 4 different ratios α (ratio of the yielding segment cross sectional area to the elastic segment cross sectional area) and β (ratio of length of the yielding segment to the total length of the core) in the frames, then the nonlinear time history analysis was performed on these frames under 7 earthquake records. Using the results of analysis, the hysteresis loop was obtained for each brace and based on which, the energy absorption demand was calculated for each brace; the results were as follows:

1. The KF value of the BRB in the bracing frame can be effective in the amount of the energy absorption demand, and the value and manner of its effect depend on the story in which the bracing is located. However, the effect of modified stiffness correction factor on the uniformity of the energy absorption demand of braces in different stories is insignificant compared to the changes in the cross-sectional area of braces in different stories.

2. The story number has a great impact on its energy absorption demand compared to the impact of different bracing KFs on its energy absorption demand.

3. The use of the BRB with higher ratios of α and β and, hence, a lower KF in the initial stories of the 5-and-10-story frames under study, led to the lower energy absorption demand for the brace designed for that story with the same core cross section, so that in the first story of the 5-story frame, when the StarBRB6.5 has been modeled with the α and β ratios of respectively 0.2 and 0.5 and KF of 1.66, its energy absorption demand has been obtained as 205.69 kN.m for the average of seven earthquake records, however when this brace has been modeled with the α and β ratios of respectively 0.3 and 0.6 and KF of 1.38, its energy absorption demand has been obtained as 198.54 kN.m.

4. In the final stories of the two 5-and-10-story frames under study, the use of BRB designed with lower α and β ratios, and hence a higher KF, created a lower energy absorption demand for that brace.

As in the fifth story of the 5-story frame, the use of StarBRB2 with the ratios α and β of respectively 0.3 and 0.6 and KF of 1.38 resulted in an energy absorption demand of 174.559 kN.m for the average of 7 earthquake records; however, the use of this brace with the ratios α and β of respectively 0.2 and 0. 5 and the KF of 1.66 led to an energy absorption demand of 165.25 kN.m for the average of 7 earthquake records.

References

AISC 341, Seismic Provisions for Structural Steel Buildings, American Institute of Steel Construction, in, Chicago, 2010.

AISC 360, Seismic provisions of structural steel building, American Institute of Steel Construction, Chicago, 2010.

ASCE/SEI 7-10, Minimum Design Loads for Buildings and Other Structures, American Society of Civil Engineers, in, United States of America, 2010.

Bosco M, Marino E, "Design Method and Behavior Factor for Steel Frames with Buckling Restrained Braces", International Association for Earthquake Engineering, 2013, 42 (8), 1243-1263.

Bruneau M, Uang C, Sabelli R, "Ductile Design of Steel Structures", McGraw-Hill, New York, 2011.

Carden LP, Itani AM, Buckle LG, "Cyclic behavior of buckling restrained braces for ductile end cross frames", Engineering Journal, American Institute of Steel Construction, 2006, 43,127-140.

Clark P, Aiken I, "Design procedures for buildings iIncorporating hysteretic damping devices", 68th Annual Convention, Santa Barbara, California, 1999.

Dehghan F, Tasnimi A, "Determination of the Parameters Influencing Behavior Factor of Buckling Restrained Braced Reinforced Concrete Frames", Amirkabir Jounrnal of Science and Research Civil and Enviromental Engineering, 2016, 48 (4), 137-142.

Dehghani E, Babaei N, Zarrineghbal A, "Investigation of the Distribution of Cumulative Ductility Demand Parameter in Various Storeys of Buckling Restrained Braced Frames", Journal of Rehabilitation in Civil Engineering, 2018.

Hosseinzadeh S, Mohebi B, "Seismic evaluation of all-steel buckling restrained braces using finite element analysis", Journal of Constructional Steel Research, 2016, 119 (Supplement C), 76-84.

Iranian National Building Code, Part 6, Structural Loadings, Ministry of Housing and Urban Development, in, Tehran, Iran 2013 (In Persian).

Iranian National Building Regulation, Part-10 , Design and Construction of Steel Buildings, Ministry of Housing and Urban Development, Tehran, Iran, 2013 (In Persian).

Jia M, Lu D, Guo L, Sun L, "Experimental research and cyclic behavior of buckling-restrained braced composite frame", Journal of Constructional Steel Research, 2014, 95, 90-105.

Jiu Jia L, Dong Y, Ge H, Kondo K, "Experimental Study on High-Performance Buckling-Restrained Braces with PerforatedCore Plates", International Journal of Structural Stability and Dynamics, 2019, 19 (1).

Karimi S, Arbabi F, "Seismic evaluation and cyclic testing of buckling restrained braces manufactured in Iran", The 14th World Conference on Earthquake Engineering, 2008, Beijing, China.

Kersting RA, Fahnestock LA, Lopez WA, Seismic Design of Steel Buckling-Restrained Braced Frames, 2015, NIST GCR, 15-917-34.

Lopez W, Sabelli R, "Seismic Design of Buckling-Restrained Braced Frames", Steel TIPS, 2004.

Mahdavipour MA, Deylami A, "Probabilistic assessment of strain hardening ratio effect on residual deformation demands of Buckling-Restrained Braced Frames", Engineering Structures, 2014, 81 (Supplement C), 302-308.

Pandikkadavath MS, Sahoo DR, "Analytical investigation on cyclic response of buckling restrained braces with short yielding core segments", International Journal of Steel Structures, 2016, 16, 1273-1285.

Qu Z, Xie J, Cao Y, Li W, "Effects of strain rate on the hysteretic behavior of buckling restrained braces", Journal of Structural Engineering, 2019, 146 (1).

Rahai AR, Alinia MM, Salehi SMF, "Cyclic performance of buckling restrained composite braces composed of selected materials", International Journal of Civil Engineering, 2009, 7 (1).

Rahnavard R, Naghavi M, Abdoli M, Suleiman M, "Investigating modeling approaches of buckling restrained braces under cyclic loads", Case Studies In Construction Marerials, 2018, 8, 476-488.

Raissi M, Foroughi AM, Eghbali M, "Effect of yielding segment on seismic performance of buckling restrained braces", Sharif Civil Engineering, 2017, 33 (2), 69-77 (In Persian).

Standard No. 2800, Iranian Code of Practice for Seismic Resistant Design of Buildings, 4th Revision, Building and Housing Research Center, Iran, 2015 (In Persian).

Watanabe A, Hitomi Y, Saeki E, Wada A, "Properties of brace encased in buckling–restraining concrete and steel tube", Ninth World Conference on Earthquake Engineering, Tokyo-Kyoto, 1988.